

Finite element analysis of piezoelectric underwater transducers for acoustic characteristics[†]

Jaehwan Kim^{1,*} and Heung Soo Kim²

¹*Department of Mechanical Engineering, Inha University, Incheon 402-751, Korea*

²*School of Mechanical and Automotive Engineering, Catholic University of Daegu, Kyungbuk 712-702, Korea*

(Manuscript Received May 13, 2008; Revised August 18, 2008; Accepted November 25, 2008)

Abstract

This paper presents a simulation technique for analyzing acoustic characteristics of piezoelectric underwater transducers. A finite element method is adopted for modeling piezoelectric coupled problems including material damping and fluid-structure interaction problems by taking system matrices in complex form. For the finite element modeling of unbounded acoustic fluid, infinite wave envelope element (IWEE) is adopted to take into account the infinite domain. An in-house finite element program is developed and technical issues for implementing the program are explained. Using the simulation program, acoustic characteristics of tonpizl transducer are analyzed in terms of modal analysis, radiated pressure distribution, pressure spectrum, transmitting-voltage response and impedance analysis along with experimental comparison. The developed simulation technique can be used for designing ultrasonic transducers in the areas of nondestructive evaluation, underwater acoustics and bioengineering.

Keywords: Finite element analysis; Underwater transducers; Tonpizl transducer; Acoustic characteristics

1. Introduction

Piezoelectric transducers are widely used to send and detect signals in many areas such as nondestructive evaluations, underwater acoustics, medical imaging and in many other ultrasonic applications. Since transducer characteristics must be predictable in the design stage, the analysis of these transducers is essential in the design to predict the performance. In the analysis of piezoelectric underwater transducers, not only the coupled behavior of the piezoelectric, but also the interaction of unbounded media as well as material damping of the transducer should be taken into account to predict accurate responses of the transducer. Generally, material damping is considered to be a proportional damping to stiffness and mass matrices

since this treatment is simple. However, proportional damping cannot properly take into account dielectric hysteresis of piezoelectric material. Thus, a more general method is necessary for the damping treatment in transducer analysis program.

To predict acoustic characteristics of piezoelectric transducers, numerical simulations are generally adopted [1-4]. For the sake of numerical simulation, the unbounded media needs to be truncated into a finite region near the transducer. However, at the truncated boundary, an artificial reflection could happen due to the presence of resonance frequencies of the truncated finite model. Thus, it is essential to accomplish a transparent boundary around the truncated boundary to escape the artificial reflection. Many attempts have been made to deal with this problem – boundary element method, infinite element, absorbing boundary conditions (ABC), Dirichlet-Neumann (DtN) method, numerical treatments based on Excitation excitation theorem, and so on [5-9]. The selection of

[†] This paper was recommended for publication in revised form by Associate Editor Maenghyo Cho

* Corresponding author. Tel.: +82 32 860 7326, Fax.: +82 32 868 1716

E-mail address: jaehwan@inha.ac.kr

© KSME & Springer 2009

unbounded domain treatment is important since numerical simulation results can be deteriorated with irregular frequencies. Since most BEMs in wave propagation problems have so-called irregular frequency, there have been several approaches to get rid of the irregular frequency – CONDOR (composite outward normal derivative overlap relation) method and CHIEF (combined Helmholtz integral equation formulation)[10, 11]. However, these methods are restricted to relatively low frequencies since many resonance modes should be taken into account in a high frequency region. Alternative treatments have been suggested based on Sommerfeld radiation condition, for example, ABC, DtN, absorbing damper, filtering scheme and so on[5-8]. In dealing with the truncated finite region, finite element modeling is usually adopted because it can easily take into account material anisotropy, material damping and geometric irregularity [9]. To easily match up the finite element model in the truncated finite region, it is natural to use infinite element at the truncated boundary since infinite element has the same interpolation behavior with the finite element. Conventional infinite element has a decaying tendency with the inverse of radial distance, which is suitable for static problems [12]. However, wave propagation problems like piezoelectric underwater transducers, there is more likely a wave behavior with decaying tendency. Infinite wave envelop element (IWEE) is suitable for wave propagation problems because it is an infinite element that has additional wave-like behavior [13].

In this paper, finite element formulation is made for piezoelectric underwater transducers by taking into account piezoelectric coupled problems along with material damping, and fluid-structure interaction. IWEE and finite elements are used to model the finite region near a piezoelectric transducer. Material damping of piezoelectric material and elastic materials is taken into account by taking the system matrices in complex form. These complex system matrices can easily include material damping of piezoelectric material as well as IWEE. However, a complex matrix solver is required. Derived formulations are implemented into an in-house program, and a tonpilz transducer is taken as an example to verify the proposed method. We once reported the program development for a piezoelectric transducer in an earlier stage [14]. This paper includes the entire development of the program, including formulation and comprehensive examples. Modal characteristics and acoustic character-

istics such as transmitting-voltage response (TVR), impedance analysis of transducers are calculated.

2. Theory

2.1 Modeling of piezoelectric underwater transducer

A schematic diagram of a piezoelectric underwater transducer is shown in Fig. 1. The piezoelectric transducer can be represented by a combination of elastic material and active material. Finite fluid, various boundary conditions and working conditions are considered around the transducer, and an infinite fluid boundary is set for the outmost of it in order to make the working conditions closer to the real world. Thus, three distinct problems are involved from the fluid-structure interaction, piezoelectric-structure coupled field and infinite fluid domain treatment. These three distinct problems are formulated separately.

Piezoelectric material is the most used active material in underwater transducers. Under the quasi-static assumption, the equations of motion for the coupled piezoelectric-structure system can be obtained by applying Hamilton’s variational principle to the piezoelectric materials. After discretizing the variables, substituting elements matrices into global matrices, the finite element formulation of coupled piezoelectric-structure system can be written as [15],

$$\begin{bmatrix} M_{UU} & 0 \\ 0 & 0 \end{bmatrix} \begin{bmatrix} \dot{U} \\ \dot{\Phi}_E \end{bmatrix} + \begin{bmatrix} D_{UU} & 0 \\ 0 & 0 \end{bmatrix} \begin{bmatrix} U \\ \Phi_E \end{bmatrix} + \begin{bmatrix} K_{UU} & K_{U\Phi} \\ K'_{U\Phi} & K_{\Phi\Phi} \end{bmatrix} \begin{bmatrix} U \\ \Phi_E \end{bmatrix} = \begin{bmatrix} F \\ Q \end{bmatrix} \quad (1)$$

where U the nodal displacement vector, Φ_E the electrical potential vector. The first term represents the inertial term, the second term damping term and the third term stiffness term. The definitions of matrices

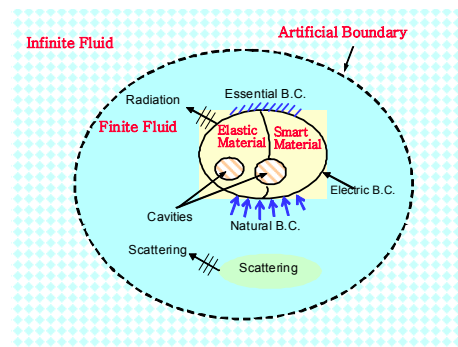


Fig. 1. Schematic diagram of piezoelectric underwater transducer.

Table 1. Matrices for fluid-structure interaction system.

Matrix	Description
$M = \int_V \rho_S N^T N dV$	The Mass Matrix of Structure
$C = \int_V k N^T N dV$	The Damping Matrix of Structure
$K = \int_V B^T C^E B dV$	The Stiffness Matrix of Structure
$Q = \int_{\Gamma_f} N^T n N_F d\Gamma$	The Area Matrix Coupled Pressure with Structural Load
$E = \frac{1}{c^2} \int_{\Omega_f} N_F^T N_F d\Omega$	The Fluid Inertia Matrix
$A = \frac{\beta}{c} \int_{\Gamma_E} N^T N d\Gamma$	The Symmetric Matrix for the Fluid where, $\beta = \frac{\gamma}{\rho c}$ γ : Characteristic Impedance of the material at the boundary
$H = \int_{\Omega_f} B_F^T B_F d\Omega$	The Fluid Stiffness Matrix
$f_1 = \int_{\Gamma_f} N^T n p_0 d\Gamma$	The Structural Force
$f_2 = \int_{\Gamma_f} N^T \frac{\partial p_0}{\partial n} d\Gamma$	The Force due to an Initial Wave Force Field

presented in Eq. (1) are all described in Table 1.

A variational principle and Galerkin's method are used for finite element discretization. Since the finite element approximates shape functions for the spatial variation of the nodal values, pressure and displacement variables can be written by shape functions and nodal values. Then, the wave equation accounting for losses at the interface boundary can be written in matrix form as [16-18],

$$E\ddot{P} + A\dot{P} + HP + \rho Q^T \ddot{U} = 0 \tag{2}$$

where A is fluid damping matrix. The definitions of matrices mentioned in this section are listed in Table 1.

The complete finite element equations for the fluid-structure interaction problem are written in assembled form as [19, 20],

$$\begin{bmatrix} M & 0 \\ \rho Q^T & E \end{bmatrix} \begin{bmatrix} \ddot{U} \\ \ddot{P} \end{bmatrix} + \begin{bmatrix} C & 0 \\ 0 & A \end{bmatrix} \begin{bmatrix} \dot{U} \\ \dot{P} \end{bmatrix} + \begin{bmatrix} K & -Q \\ 0 & H \end{bmatrix} \begin{bmatrix} U \\ P \end{bmatrix} = \begin{bmatrix} f_1 \\ f_2 \end{bmatrix} \tag{3}$$

This is a coupled structure-pressure equation. The second term represents the damping term. Note that this is an unsymmetric matrix equation, which consumes a great deal of computational resources. An alternate formulation for the wave equation is in

Table 2. Matrices for piezoelectric-structure coupled system.

Matrix	Description
$M_{UU} = \int_V \rho_S N^T N dV$	The Kinematical Constant Mass Matrix
$K_{UU} = \int_V B^T c^E B dV$	The Elastic Stiffness Matrix
$K_{U\Phi} = \int_V B^T e^T B_E dV$	The Piezoelectric Coupling Matrix
$K_{\Phi\Phi} = \int_V B_E^T \epsilon^S B_E dV$	The Dielectric Stiffness Matrix
$D_{UU} = a \int_V \rho_S N^T N dV + b \int_V B^T c^E B dV$	The Damping Matrix a, b : damping coefficients
$F = \int_V N^T N_{FB} f_B dV + \int_{\Gamma} N^T N_{FS} f_S d\Gamma + N^T f_P$	External Force : Body Force, Surface Force, Point Force
$Q = - \int_{\Gamma} N_E^T N_{QS} q_S d\Gamma - N_E^T q_P$	Electrical Charge : Surface and Point Electrical Charge

terms of a velocity potential. One can consider velocity u as the gradient of a scalar potential ϕ . Following the same derivation as shown above, the finite element formulation of the coupled fluid-structure system based on velocity potential can be obtained as [19],

$$\begin{bmatrix} M & 0 \\ 0 & -\rho E \end{bmatrix} \begin{bmatrix} \ddot{U} \\ \ddot{\Phi} \end{bmatrix} + \begin{bmatrix} C & \rho Q \\ \rho Q & -\rho A \end{bmatrix} \begin{bmatrix} \dot{U} \\ \dot{\Phi} \end{bmatrix} + \begin{bmatrix} K & 0 \\ 0 & -\rho H \end{bmatrix} \begin{bmatrix} U \\ \Phi \end{bmatrix} = \begin{bmatrix} f_1 \\ g_2 \end{bmatrix} \tag{4}$$

where Φ the velocity potential vector and $g_2 = \int_0^t f_2 dt$.

The velocity potential provides symmetry of equations of motion and computational efficiency. However, difficulties occur when applying boundary conditions because velocity potential is not a physical quantity. The definitions of matrices mentioned in this section are listed in Table 2.

2.2 Treatment of infinite fluid domain

When an infinite fluid region is truncated into a finite region, a non-reflecting boundary condition should be provided on the truncated boundary to eliminate the artificial reflections arising at the boundary. Since the infinite wave envelope element (IWEE) has additional wave behavior, the use of IWEE is more suitable than conventional infinite element for the acoustic analysis of underwater transducers [13, 21]. Thus, IWEE is used to deal with infinite domain around the transducers. IWEE has three distinct characteristics: a mapping function that maps

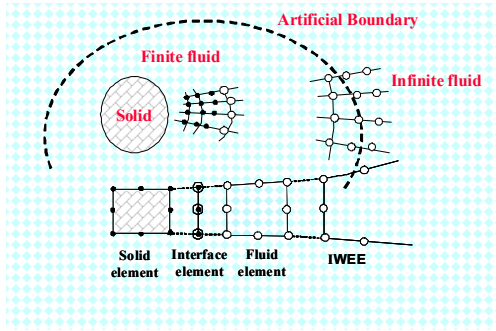


Fig. 2. Schematic diagram of IWEE with finite element model.

the real coordinate to an infinite domain, a shape function that has a decaying tendency and wave-like behavior, and a modified weighting function for Galerkin's formulation. Fig. 2 represents the concept for infinite domain modeling by using finite element and IWEE. The finite element equation for IWEE is similar to that of conventional fluid elements except for some differences in shape function and weighting function. Detailed derivation can be found in the reference [13].

The shape function of IWEE is a product of the shape functions in s and t coordinates,

$$N_i^n(s,t) = T_i^n(t)S_1(s)e^{-ik\mu(s,t)}, \quad 1 \leq i \leq n \quad (\text{edge 1}) \tag{5}$$

$$N_{n+1}^n(s,t) = T_i^n(t)S_2(s)e^{-ik\mu(s,t)}, \quad 1 \leq i \leq n \quad (\text{edge 2})$$

The shape functions in t -coordinate are written with Lagrangian polynomials:

$$T_i^n(t) = \frac{\pi(t)}{\pi'(t_i)(t-t_i)}, \quad 1 \leq i \leq n \tag{6}$$

where
$$\pi(t) = \prod_{i=1}^{n+1} (t-t_i)$$

And, the shape functions in s -coordinate are:

$$S_1(s) = \frac{1+s}{2}, \quad S_2(s) = \frac{1-s}{2} \tag{7}$$

Weighting function for IWEE uses its complex conjugate of the shape function to eliminate exponential terms in mass and stiffness matrices of IWEE, which results in reducing computation load. Thus,

$$W^n(s,t) = G(t)N^n(s,t) = G(t)T^n(t)S(s)e^{+ik\mu(s,t)} \tag{8}$$

where geometric weighting factor, $G(t) = \left(\frac{1-t}{2}\right)^2$.

Then, the stiffness, mass and force matrices of IWEE are

$$K_{ij} = \int_V \nabla W_i \cdot \nabla N_j dV \tag{9}$$

$$M_{ij} = \int_V \frac{1}{c^2} W_i N_j dV \tag{10}$$

$$F_i = -i\omega \int_{S_{body}} \rho W_i \bar{v} dS \tag{11}$$

Above element matrices use a modified Galerkin's method, which results in non-symmetric matrix and includes complex terms.

2.3 Modal analysis

When a harmonic excitation is given, the finite element Eq. (1) for the coupled piezoelectric-structure system becomes

$$\begin{bmatrix} K_{UU} - \omega^2 M_{UU} & K_{U\Phi} \\ K'_{U\Phi} & -K_{\Phi\Phi} \end{bmatrix} \begin{bmatrix} U \\ \Phi_E \end{bmatrix} = \begin{bmatrix} 0 \\ Q \end{bmatrix} \tag{12}$$

The frequency ω represents the harmonic driving frequency. The mechanical forces are set to zero, and material damping is included in the stiffness matrix in complex form. Electrical potential variable has three parts: hot electrode, ground electrode and internal potential dof in the piezoelectric material. Once the internal potential dof are eliminated from the system equations by static condensation, then the system equations can be written as,

$$\begin{bmatrix} \bar{K}_{UU} - \omega^2 M_{UU} & \bar{K}_{U\Phi} \\ \bar{K}'_{U\Phi} & -\bar{K}_{\Phi\Phi} \end{bmatrix} \begin{bmatrix} U \\ \Phi_0 \end{bmatrix} = \begin{bmatrix} 0 \\ I/j\omega \end{bmatrix} \tag{13}$$

where Φ_0 is the given electrical potential at the 'hot' electrode. Charge Q is replaced with $I/j\omega$, where I is the input current. Note that the potential and the dielectric stiffness matrices are now scalar quantities. Here, the matrices with bars indicate the condensed

results.

Eq. (14) gives a direct expression of the terminal admittance Y in terms of the various electro-elastic stiffness properties:

$$Y = \frac{I}{\Phi_0} = j\omega[-\bar{K}_{\Phi\Phi} - \bar{K}'_{U\Phi}(\bar{K}_{UU} - \omega^2 M_{UU})^{-1} \bar{K}_{U\Phi}] \quad (14)$$

At resonance, $Y \rightarrow \infty$ so $\Phi_0 \rightarrow 0$ for $I \neq 0$. Thus, regardless of $\bar{K}_{U\Phi}$ and $\bar{K}_{\Phi\Phi}$, it gives

$$(\bar{K}_{UU} - \omega^2 M_{UU})U = 0 \quad (15)$$

Therefore, $\det(\bar{K}_{UU} - \omega^2 M_{UU}) = 0$ gives the eigenvalues ω_i and corresponding eigenvectors U_i of the i -th resonance mode. At anti-resonance, $Y \rightarrow 0$ and so $I \rightarrow 0$ for $\Phi_0 \neq 0$, which gives

$$\left(\bar{K}_{UU} + \frac{\bar{K}_{U\Phi} \cdot \bar{K}'_{U\Phi}}{\bar{K}_{\Phi\Phi}} - \omega^2 M_{UU} \right) U = 0 \quad (16)$$

where the determinant will give the eigenvalue ω_i and corresponding eigenvector U_i of the i -th anti-resonance mode [21]. The resonance mode corresponds to an electrical short circuit condition, while the anti-resonance mode does to open circuit condition.

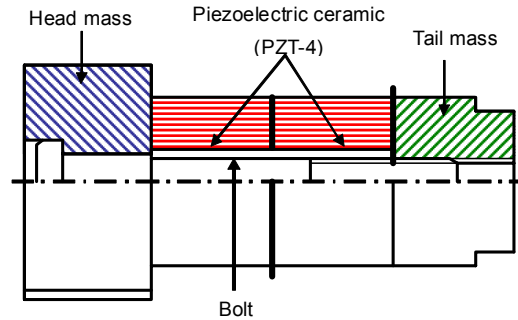
3. Numerical results and discussion

3.1 2-D modeling of tonpizl transducer

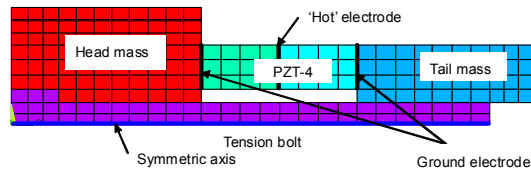
Fig. 3(a) shows the finite element model of a typical tonpizl transducer that consists of two piezoelectric ceramics sandwiched between head mass and tail mass, and tension bolt ensuring intimate mechanical contacts between components. The head mass is circular and gives the transducer a radiation face. PZT-4 is used for the piezoelectric ceramics. Four-node quadrilateral axisymmetric elements are used to model the tonpizl transducer as shown in Fig. 3(b). Total 193 linear elements and 240 nodes are used in the model. The two adjacent piezoelectric ceramics are assembled to have opposite poling direction. The piezoelectric stacks will both expand away from their common face or contract toward that face, depending on the polarity of the applied voltage. Symmetric boundary conditions along the radial direction are specified at the center line and at the outside of the head mass due

Table 3. Material properties of the tonpizl transducer.

	Young's modulus (GPa)	Density (kg/m ³)	Poisson's ratio
Head mass	70.3	2770	0.33
Tail mass	206.0	7955	0.30
Bolt	185.0	7920	0.30
Piezoceramic	PZT-4		



(a) Tonpizl transducer



(b) Finite element model

Fig. 3. Structure of tonpizl transducer and its 2-D axisymmetric finite element model.

to the repeated unit of tonpizl elements. The back side of the head mass is fixed along the axial direction. Three electrodes are placed on the three major surfaces of these ceramics for giving excitations or making measurements. The material properties are listed in Table 3.

Fig. 4 shows the 2-D axisymmetric finite element model of tonpizl transducer in water. Total 382 linear elements and 444 nodes are made in the model. The detailed structure of tonpizl transducer is the same as shown in Fig. 3. To model an infinite fluid, the fluid adjacent to the piezoelectric transducer is modeled by using conventional fluid element, and on the mathematical boundary just outside of the finite fluid, IWEE is used as shown in Fig. 4.

3.2 Finite element program

The finite element formulation for piezoelectric un-

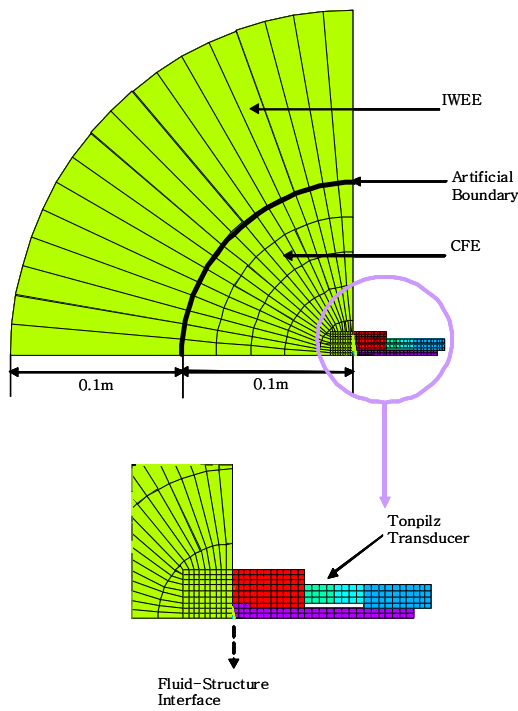


Fig. 4. 2-D axisymmetric finite element model of the tonpilz transducer in water.

derwater transducers was implemented into an in-house FORTRAN program. This program can support any combination of linear elements in terms of axisymmetric element, fluid element, piezoelectric element, IWEE in two-dimensions as well as three-dimensions. Complex system matrices are used to take into account the material damping in the piezoelectric material as well as structural material. Material damping in acoustic window material is important in predicting the acoustic performance of underwater transducers. To reduce computation time and memory space, the global system matrices are constructed into symmetrically banded form by arranging each node's dof in a row [15]. To solve the global system matrix equation in harmonic analysis, several solvers are supported: skyline solver, half Gaussian elimination solver, LU decomposition solver.

For the modal analysis, ARPACK solver is used [22]. As pre and post processors of the developed program, commercial pre and post processors such as ANSYS or Pro-Engineer can be used.

3.3 Modal analysis of tonpilz transducer

In the modal analysis of piezoelectric transducers,

Table 4. Comparison of natural frequencies of the tonpilz transducer (Normalized with respect to the first resonance of ANSYS result).

Mode	Current program (Hz)	ANSYS (Hz)	Rel. Error (%)
1st	(0.517, 0.000i)	0.512	1.0
2nd	(1.045, 0.000i)	1.000	4.45
3rd	(1.338, 0.000i)	1.321	1.3
4th	(1.629, 0.000i)	1.609	1.2
5th	(2.215, 0.000i)	2.123	4.4

short and open circuit cases should be taken into account, which span the extremes of the piezoelectric coupling effect on the voltage and displacement. For the short circuit case that is commonly called 'resonance' condition, a zero voltage is applied at the electrodes, where all voltage potentials are connected in common. In the open circuit case that is called 'anti-resonance', ground voltage is applied at the outer electrode of the ceramic stack; meanwhile no voltage is specified at the rest electrodes. Table 4 shows five natural frequencies for short circuited tonpilz transducer. These frequencies were normalized with respect to the second resonance frequency (ANSYS result). Since the system matrices are complex, the natural frequencies are given in complex form. However, imaginary parts of the frequencies are so small compared with real parts. Imaginary part of the complex natural frequencies represents decaying wave behavior on the transducer. Comparison is made with results obtained from the commercial package, ANSYS. Figure 5 shows these five mode shapes obtained from the current program and ANSYS. The first and second modes are important for efficiently radiating and receiving signals. A comparison of natural frequencies and mode shapes shows good agreement between the current modeling method and the commercial package, ANSYS.

3.4 Acoustic characteristic analysis of tonpilz transducer in water

To find the acoustic characteristics of the transducer, a harmonic analysis was performed. The input for this simulation is unit voltage imposed across the 'hot' electrodes of the transducer at the central electrode. The input potential is 1 V at the central electrode, while the first and third electrodes are set to 0 V for ground. A harmonic analysis is performed over

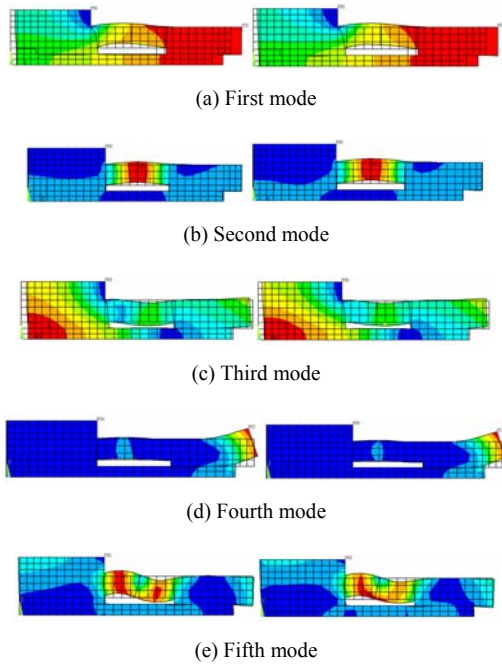


Fig. 5. Comparison of mode shapes of the tonpilz transducer (short circuit).

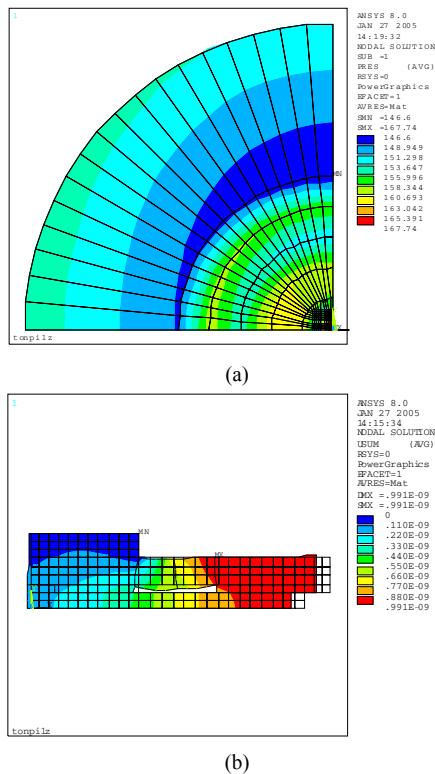


Fig. 6. Pressure distribution in the water (a) and deformed shape of the tonpilz transducer (b).

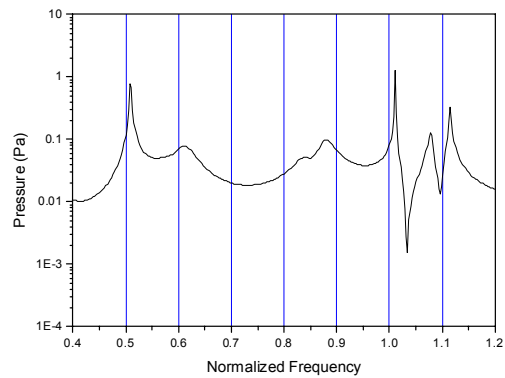


Fig. 7. Pressure spectrum of the tonpilz transducer.

a frequency range. At each frequency, the program computes the steady-state response of the transducer. Fig. 6(a) shows the pressure distribution in water, and (b) the deformed shape of the transducer at the first resonant frequency. Note that since ANSYS was used for the post processor, its name appeared. As the transducer vibrates, pressure waves propagate into the water uniformly. The pressure spectrum can be found at a specific point in the fluid. A point was selected in the fluid region, as shown in Fig. 4(a), which was on the acoustical axis of the tonpilz transducer. The pressure was calculated at this point with a frequency sweep.

Fig. 7 shows the pressure spectrum at the point. The first and second resonance peaks can be seen from the pressure spectrum. The transmitting-voltage response (TVR) of a transducer is the pressure produced at a point 1 meter far from the transducer in the direction of the axis of its beam pattern by a unit voltage into the transducer. From the pressure spectrum at the selected point on the acoustical axis, TVR was found in decibels relative to 1 micro Pascal as 1 Pa/V.

Fig. 8 shows the TVR results. The simulated TVR was compared with an experimental result. The experimental test was performed in an underwater testing facility in Korea. RF pulse was generated from an RF pulse generator and fed to a projector submerged in the underwater testing facility. Conventional pulse echo technique was used to test the transducer performance. The measured TVR shows a broad peak near the second resonance while the simulated TVR peak is sharp near it. This is due to the fluid loading effect in the experiment, but the simulation result showed this effect to be small.

It is well known that the input impedance of a piezoelectric transducer represents the dynamic behavior

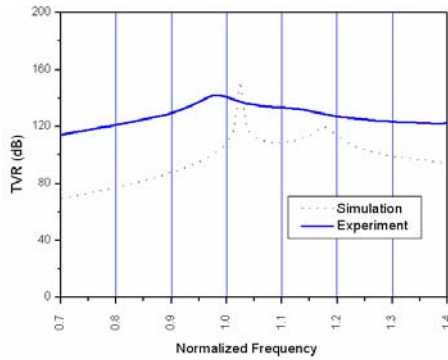


Fig. 8. TVR of the tonpilz transducer.

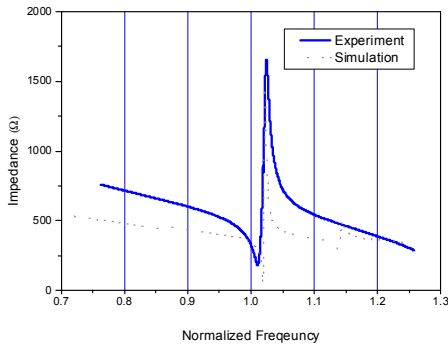


Fig. 9. Impedance of the tonpilz transducer.

of the transducer very accurately. Thus, the impedance of the tonpilz transducer is calculated. When a unit voltage is applied on the ‘hot’ electrode, the input electrical impedance can be written as $Z = V/I = 1/I = 1/j\omega \sum Q_i$.

Here, ω is the operating frequency, j is $\sqrt{-1}$ and $\sum Q_i$ is the summed point charge at the electrode. The point charge Q_i can be found from the second part of Eq. (14) by applying 1 volt on the ‘hot’ electrode. Impedance is a complex number and can be represented as,

$$Z = R + iX = |Z|e^{j\phi} \tag{17}$$

where Z impedance, R resistance, X reactance, $|Z|$ the magnitude of impedance and ϕ the phase of impedance. Fig. 9 shows the impedance of the tonpilz transducer. Comparison is made with an experimental result. The impedance measurement was made on the transducer in air by using an HP 4192A impedance analyzer. The amplitude of the impedance decreased and suddenly increased near the resonance and anti-resonance frequencies. Peaks occurred near the corresponding resonance frequency shown on the TVR.

Note that the simulated peak is sharper than the experimental peak. This is due to under-estimation of fluid loading on the transducer from the simulation. Nevertheless, the simulation can predict the experimental result. Thus, the proposed simulation technique is useful to predict the acoustic characteristics of tonpilz transducers. However, more efforts should be devoted in the program development to deal with large sized models for real applications and reducing computational burden.

4. Conclusions

A simulation technique of a piezoelectric underwater transducer was presented by taking into account wave radiation. Finite element formulation was derived for the coupling of piezoelectric and elastic materials as well as fluid-structure interaction.

IWEE was introduced at the truncated boundary to deal with the infinite domain of the fluid. The tonpilz transducer was taken as a numerical example, and two-dimensional finite element modeling was performed. Modal and harmonic analysis were conducted to validate the simulation technique. Comparison of natural frequencies and mode shapes with the results of a commercial finite element program showed a good correlation. To demonstrate the simulation capabilities for acoustic characteristics of piezoelectric transducers, radiated pressure distribution in water was found, and the pressure spectrum was calculated. From the pressure calculation, a TVR was simulated and the simulated peak was sharper than the experimental peak. For further verification, the input impedance of the transducer was simulated. The developed simulation technique can be used for designing ultrasonic transducers in the areas of non-destructive evaluation, underwater acoustics and bioengineering.

Acknowledgment

This work was supported by Creative Research Initiatives (EAPap Actuator), KOSEF/MEST.

References

- [1] H. Allik, K. M. Webman and J. T. Hunt, Vibration response of sonar transducer using piezoelectric finite elements, *J. Acoust. Soc. Am.* 87 (1990) 1861-1867.
- [2] R. Lerch, Simulation of piezoelectric devices by

- two- and three-dimensional finite elements, *IEEE Trans. Ultrason. Ferroelectr. Freq. Control* 37 (1990) 233-247.
- [3] J. A. Hossack and G. Hayward, Finite element analysis of 1-3 composite transducers, *IEEE Trans. Ultrason. Ferroelectr. Freq. Control* 38 (1991) 618-627.
- [4] H. Allik and T. J. R. Hughes, Finite element method for piezoelectric vibration, *Int. J. Num. Meth. Eng.* 2 (1970) 151-157.
- [5] B. Engquist and A. Majda, Radiation boundary conditions for acoustic and elastic wave calculations, *Comm. Pure. Appl. Math.* 32 (1979) 313-357.
- [6] S. Liapis, Method for suppressing the irregular frequencies from integral equations in water-structure interaction problem, *Comput Mech.* 12 (1993) 59-68.
- [7] A. Bayliss and E. Turkel, Radiation boundary conditions for wave-like equations, *Comm. Pure. Appl. Math.* 33 (1980) 707-725.
- [8] D. Givoli and J. B. Keller, Non-reflecting boundary conditions for elastic waves, *Wave Motion* 12 (1990) 261-279.
- [9] J. Kim, V. V. Varadan and V. K. Varadan, Finite element modeling of scattering problems involving infinite domains using drilling degrees of freedom, *Comput. Methods Appl. Mech. Eng.* 134 (1996) 57-70.
- [10] A. J. Burton and G. F. Miller, The application of integral equation methods to the numerical solution of some exterior boundary value problems, *Proc. R. Soc. London, Ser. A* 323 (1971) 201-210.
- [11] H. A. Schenck, Improved integral formulation for acoustic radiation problems, *J. Acoust. Soc. Am.* 44 (1968) 41-58.
- [12] P. Bettess, Infinite elements, *Int. J. Numer. Methods Eng.* 11 (1977) 53-64.
- [13] L. Cremers, K. R. Fyfe and J. P. Coyette, A variable order infinite acoustic wave envelope element, *Journal of Sound and Vibration* 171 (1994) 483-508.
- [14] J. Kim, E. Jung and S.-B. Choi, Radiation and scattering analysis of piezoelectric transducer using finite and infinite wave envelop element *SPIE's 9th Annual Symposium on Smart Structures and Materials*, San Diego, CA, USA. 4693 (2002) 607-613
- [15] V. V. Varadan, J. Kim, V. K. Varadan, Modeling of piezoelectric sensor fidelity. *IEEE Trans. Ultrason. Ferroelectr. Freq. Control* 44 (1997) 538-547.
- [16] O. C. Zienkiewicz, P. Bettess, Fluid-structure dynamic interaction and wave force: An introduction to numerical treatment. *Int. J. Numer. Methods Eng.* 13 (1978) 1-16.
- [17] A. D. Pierce, *Acoustics, An Introduction to its Physical Principles and Applications*, McGraw-Hill, New York, USA, (1981).
- [18] G. C. Everstine, A Symmetric potential formulation for fluid-structure interaction, *Journal of Sound and Vibration* 79 (1981) 157-160.
- [19] G. C. Everstine, Finite element formulations of structural acoustics problems. *Computers & Structures* 65 (1997) 307-321.
- [20] M. C. Junger, D. Feit, *Sound, Structures, and Their Interaction*, 2nd Edition, MIT Press, Cambridge, MA, 1986.
- [21] D. W. Hawkins and P. T. Gough, Multiresonance design of a tonpiliz transducer using the finite element method, *IEEE Trans. Ultrason., Ferroelectr. Freq. Control* 43 (1996) 782-790.
- [22] <http://www.caam.rice.edu/software/ARPACK/index.html>.



Jaehwan Kim received his B.S. degree in Mechanical Engineering from Inha University, in 1985. He received his M.S. degree from KAIST in 1987 and his Ph.D. degree from The Pennsylvania State University in 1995. Dr. Kim is currently a Professor

of the Dept. of Mechanical Engineering at Inha University, Inchoen, Korea. He serves as an Associate Editor of Smart Materials and Structures. He is the director of Creative Research Center for EAPap Actuator supported by KOSEF. Dr. Kim's research interests are smart materials such as piezoelectric materials, electroactive polymers and their applications including sensors, actuators, motors and MEMS devices.



Heung Soo Kim received his B.S. and M.S. degrees in the Department of Aerospace Engineering from Inha University, Korea in 1997 and 1999, respectively. He obtained his Ph. D degree in the Department of Mechanical and Aerospace Engineering from Arizona State University in 2003. He is now working as an assistant professor in the School of Mechanical and Automotive Engineering, Catholic University of Daegu. His main research interests are in biomimetic actuators and sensors, structural health monitoring, smart materials and structures as applied to aerospace structures and vehicles.